Research Article

Nan Li, Zhenhe Zhai*, Jian Ma, Bin Guan, Wenhui Cui, and Duan Li

Ka/C dual frequency ranging system for ocean altimetry satellite and analysis of ionospheric error

https://doi.org/10.1515/astro-2022-0220 received December 29, 2022; accepted April 06, 2023

Abstract: In view of the future development trend of ocean altimetry satellites, the design idea of Ka/C dual frequency combination system is proposed, that is, the mode of using an altimeter antenna to contain Ka and C frequencies (35.7 and 5.3 GHz, respectively) for combined ranging. First, the random error model of altimeter measuring the distance from the altimeter phase center to the sea surface is given, and the analysis shows that the ionospheric correction error is one of the important factors. Second, the calculation of typical ionospheric parameters shows that the influence of ionospheric higher order terms on altimeter ranging is below the mm level, and its influence can be ignored. The rigorous expression for the first-order and second-order term correction of ionosphere error are given, respectively, by using dual frequency and three frequencies. The computational experiment of Jason-2 and SARAL satellite show that the maximum magnitude of ionospheric error correction in Ku band can reach 11 cm, while the maximum magnitude of ionospheric error correction in Ka band can reach 2 cm. For high-precision applications, ionospheric corrections must be made for single Ka frequency. After Ka/C dual frequency combination is adopted, error correction can be directly conducted without global ionospheric map (GIM) model, and its accuracy will be further improved than GIM model. Under 1Hz sampling

Duan Li: State Key Laboratory of Geo-information Engineering,

Beijing, China, e-mail: liduan_cug@126.com

conditions, the ionospheric correction accuracy of Ka/C combination can be better than 2.5 mm, basically eliminating the influence of the ionosphere, and the total ranging accuracy can reach 3.5 cm considering the propagation error.

Keywords: satellite altimetry, ionospheric error, Ka/C dual frequency combination, SARAL satellite

1 Introduction

Ocean satellite altimetry technology (including synthetic aperture radar and traditional bottom looking radar mode) is an important means to obtain global sea level changes, wind fields, gravity fields, and seabed topography. Dozens of altimetry satellites have been launched for oceanography, geodesy, and other scientific research (Abdalla et al. 2021, Cheng et al. 2019, Huang et al. 2007, Roblou et al. 2011, Sandwell et al. 2014, Vignudelli et al. 2019, Nguyen et al. 2020). With the continuous development of technology, high-resolution, high-precision, and high timeliness will become the trend of future ocean satellite altimetry. In order to eliminate the impact of the ionosphere on high-precision satellite altimetry products, currently two methods are commonly used for ionospheric correction (Azpilicueta and Nava 2021, Ablain et al. 2019, Quilfen and Chapron 2021, Schwatke and Dettmering 2022). One is using dual frequency ranging correction, and the other is using the global ionospheric map (GIM) model from terrestrial dual-frequency Global Navigation Satellite Systems measurements (Borries et al. 2020).

At present, the commonly used altimeters for satellite altimetry generally use the Ku/C dual frequency system. Taking the Jason-3 satellite as an example, its 1 Hz ranging accuracy in the Ku band can reach 1.8 cm. Although the use of the Ku/C dual frequency system can reduce the impact of ionospheric errors, at present, 100 km and above post-processing data filtering scales are widely used (Jin *et al.* 2012) just because the residual error is still large, which is not the optimal strategy in theory for

^{*} Corresponding author: Zhenhe Zhai, State Key Laboratory of Geoinformation Engineering, Beijing, China, e-mail: wuji41@163.com Nan Li: State Key Laboratory of Astronautic Dynamics, Xi'an Satellite Control Center, Xi'an, China, e-mail: 82520725@qq.com Jian Ma: State Key Laboratory of Geo-information Engineering, Beijing, China, e-mail: majian_19881006@163.com Bin Guan: State Key Laboratory of Geo-information Engineering, Beijing, China, e-mail: pershingb@aliyun.com Wenhui Cui: State Key Laboratory of Astronautic Dynamics, Xi'an Satellite Control Center, Xi'an, China, e-mail: cwenh_80@163.com

Nan Li et al.

1-2 km high-resolution marine surveying and mapping. Some satellite, such as the SARAL satellite which carried the AltiKa altimeter use the single frequency Ka system, and its Ka band with 1 Hz ranging accuracy can reach 1 cm (Dhote et al. 2021, Verron et al. 2015, Jing et al. 2016, Pirooznia et al. 2016, Ghosh et al. 2017, Yang et al. 2017), and for offshore and sea ice, measurement accuracy is higher than the Ku band, while the sea ice area can account for up to 8% of the global total ocean area (Yang et al. 2013, Denise et al. 2015). Although Ka band is slightly affected by the ionosphere, it cannot completely eliminate the influence of ionospheric delay error (Tournadre et al. 2009a, b). In view of the shortcomings and development trend of the existing ocean satellite altimetry system, this study proposes a Ka/C dual frequency combined ranging system and analyzes its applicability from the perspective of ionospheric error.

2 Random error model for altimeter to measure the distance from altimeter to sea surface

The spaceborne altimeter measures the vertical distance from the altimeter phase center to the sea surface. According to the altimeter system principle, the distance error between the altimeter and the sea surface includes: original ranging value error, retracking correction value error, ionosphere and sea state deviation caused by the influence of propagation environment, errors related to measurement frequency, and some dry and wet tropospheric errors and tidal errors unrelated to frequency. According to the above analysis, the random error of the distance from the altimeter to the sea surface can be defined as follows:

$$m(R) = \sqrt{m(\text{alt})^2 + m(\text{ret})^2 + m(\text{ion})^2 + m(\text{ssb})^2},$$

$$+ m(\text{tro})^2 + m(\text{tide})^2$$
(1)

where m(R) represents the random total error of the distance from the altimeter phase center to the sea surface, m(alt) represents the ranging error of the altimeter itself, m(ret) represents the waveform retracking error, m(ion) represents the ionospheric correction error, m(tro) represents the tropospheric correction error, and m(tide) represents the tropospheric correction error, and m(tide) represents the tidal correction error. m(alt) is determined by the performance of the instrument itself. Under the condition that the mathematical model of echo waveform is fixed, m(ret) can be better than 1 cm m(ion) which needs to be analyzed according to the correction model. Usually, m(ssb) is corrected by a multi

parameter model containing significant wave height and wind speed, and the correction accuracy reaches 2 cm (Haoran and Hongli 2013). In m(tro), the dry tropospheric error is generally corrected by model, and the wet tropospheric error is corrected by atmospheric correction radiometer, with a total correction accuracy of 1.5 cm (Wang et al. 2013). m(tide) is usually corrected by the global tide model (including ocean tide, solid tide, and polar tide), and the correction accuracy reaches 2 cm (Turner et al. 2013). It should be emphasized that Eq. (1) describes the ranging error obtained at the same measurement time and at the same measurement sampling frequency. That is, all errors should be analyzed under the same sampling frequency. For traditional altimeter products, the sampling frequency is usually 1 Hz (about 5-7 km). For synthetic aperture radar altimeter products, the sampling interval can be up to 300 m. The spatial variation scale of the troposphere is more than 20 km, which has little impact on the current altimeter measurement resolution. The resolution of typical tidal models, such as Final Element Solution (FES) 2014, has also reached 0.06° (Fan 2019), which can basically meet the requirements of high-resolution altimetry. From the above analysis, it can be seen that in order to form a matching relationship with all errors, the ionospheric correction must consider the changing scale with higher resolution. From the current research, the spatial change in the ionosphere is more complex, and different latitudes and altitudes will have different changes. At present, the widely used 100 km filtering scale in satellite altimetry has lost the opportunity to correct the fine ionosphere while reducing the ionospheric error. Therefore, it is not the best choice. In view of this, we will focus on the correction model and error of ionospheric influence.

3 Ionospheric 1-3 order term influence analysis

Theoretically, the dual frequency correction can eliminate the influence of the ionospheric first-order term. However, for satellite altimetry, whether the influence of ionospheric second-order and third-order terms should be considered in the analysis of few literatures. This paper analyzes based on the 1–3 order term expression of ionospheric correction given by Marques HA (Marques *et al.* 2011) as follows:

$$I^{(1)} = -\frac{A}{2f^2} \cdot \text{TEC},\tag{2}$$

$$I^{(2)} = \frac{eA}{f^3 2\pi m_e} ||B|| \cdot |\cos \theta| \cdot \text{TEC}, \tag{3}$$

$$I^{(3)} = \frac{3A^2}{8f^4}\eta \cdot N_{e,\text{max}} \cdot \text{TEC},$$
 (4)

where $I^{(1)}$, $I^{(2)}$, and $I^{(3)}$, respectively, represent the 1–3 order terms of ionospheric correction, f represents the signal frequency, $A \approx 80.6 \text{ m}^3/\text{s}^2$, $e = 1.60218 \times 10^{-19}$. Total electron content (TEC) represents the total electron content in the propagation path, $N_{e, \text{max}}$ represents the maximum electron density, and η is generally 0.66. m_e represents the electronic mass, and the value is 9.10939×10^{-31} kg, ||B|| represents the geomagnetic induction vector, θ represents the angle between electromagnetic wave signal and geomagnetic field. Since the article mainly discusses the magnitude of ionospheric error, therefore, the geomagnetic field strength $||B|| \cdot |\cos \theta|$ can be simplified as the average geomagnetic field strength on the propagation path, and the value is 40,000 nT in this study. The Ka band (35.7 GHz), C band (5.3 GHz), and Ku band (13.57 GHz) commonly used in satellite altimetry are analyzed as follows. The typical TEC values are derived from the ionospheric time variation (Tariku 2015), and the maximum value is 87.5TECU, the minimum value is 9.7TECU in this study. $N_{e, \text{max}}$ uses the typical values given in literature (Borries et al. 2020). Table 1 shows the 1-3 order magnitude of ionospheric terms of each frequency calculated with the above values.

It can be seen from Table 1 that, under typical parameters, the ionospheric error of frequency band C is larger than that of the other two frequency bands, with the maximum of 1.2 m. The ionospheric first-order term of frequency band Ku is about 2cm at least and 20cm at most. Even the Ka frequency band which is insensitive to the ionosphere will have an error of 2 cm under specific conditions. Obviously, for high-precision ocean altimetry, a single frequency altimeter is not the best choice. On the other hand, unlike the ionospheric error characteristics under GPS and other satellite navigation systems (Wang and Wu 2005), the ionospheric second-order and thirdorder terms in Ku, Ka, and C bands are smaller than mm. Therefore, for the current commonly used ocean satellite altimeter, when only the 1 cm precision ranging magnitude is considered, the ionospheric second-order and third-order

terms do not need to be considered, and the correction of the ionospheric first-order terms should be focused.

4 Mathematic model of double frequency ionospheric error correction to first-order term

At present, the main purpose of most altimeters using the dual frequency system is to eliminate the ionospheric influence. The exact description is to eliminate the ionospheric first-order term influence. In order to distinguish the difference from the GPS ionospheric correction (Olivier and Paul 2004, Wang and Wu 2005, Brunner and Gu 1991, Imel 1994, Zhang *et al.* 2018), this work will derive the ionospheric correction model of satellite altimetry in detail. According to the principle of electromagnetic wave propagation, the functional relationship between the code velocity refractive index $n_{\rm g}$ and the phase velocity refractive index $n_{\rm p}$ can be expressed as follows:

$$n_{\rm g} = \frac{n_{\rm p}}{1 - f \frac{1}{n_{\rm p}} \frac{{\rm d}n_{\rm p}}{{\rm d}f}}.$$
 (5)

Considering the first and second-order terms, the expansion is as follows:

$$n_{\rm g} = n_{\rm p} \left[1 + f \frac{1}{n_{\rm p}} \frac{\mathrm{d}n_{\rm p}}{\mathrm{d}f} + f^2 \frac{1}{n_{\rm p}^2} \left(\frac{\mathrm{d}n_{\rm p}}{\mathrm{d}f} \right)^2 \right].$$
 (6)

The phase velocity refractive index discretization expression (including second-order term) is as follows:

$$n_{\rm p} = 1 + \frac{a_1}{f^2} + \frac{a_2}{f^3} + \cdots.$$
 (7)

where a_1,a_2 represent 1st and 2nd order coefficients. Consider $n_{\rm g}$ the second order-term and substitute $n_{\rm p}$ (including the second-order term)

$$n_{\rm g} = 1 - \frac{a_1}{f^2} - 2\frac{a_2}{f^3} + \frac{1}{1 + \frac{a_1}{f^2} + \frac{a_2}{f^3}} \left(4\frac{a_1^2}{f^4} + 12\frac{a_1a_2}{f^5} + 9\frac{a_2^2}{f^6} \right). \tag{8}$$

Table 1: Order of 1-3 ionospheric terms at various frequencies (m)

Constant parameter	Single frequency	First-order term	2nd order term	3rd order term
TEC = 87.5TECU, $N_{e,\text{max}} = 20 \times 10^{12}$	Ku band	-0.192	-1.57×10^{-5}	-8.25×10^{-7}
	Ka band	-0.027	-8.61×10^{-7}	-1.71×10^{-8}
	C band	-1.251	-2.64×10^{-4}	-3.55×10^{-5}
TEC = 9.7TECU , $N_{e,\text{max}} = 6 \times 10^{12}$	Ku band	-0.023	-1.78×10^{-6}	-2.81×10^{-8}
	Ka band	-0.003	-9.74×10^{-8}	-5.83×10^{-10}
	C band	-0.142	-2.99×10^{-5}	-1.21×10^{-6}

From the above equation, the code and phase changes in the electromagnetic signal in dissipative medium can be expressed as follows:

$$\delta_{g} = \int \begin{pmatrix} -\frac{a_{1}}{f^{2}} - 2\frac{a_{2}}{f^{3}} + \frac{1}{1 + \frac{a_{1}}{f^{2}} + \frac{a_{2}}{f^{3}}} \\ \left(4\frac{a_{1}^{2}}{f^{4}} + 12\frac{a_{1}a_{2}}{f^{5}} + 9\frac{a_{2}^{2}}{f^{6}} \right) \end{pmatrix} ds, \tag{9}$$

$$\delta_{\rm p} = \int \left(\frac{a_1}{f^2} + \frac{a_2}{f^3}\right) \mathrm{d}s. \tag{10}$$

It can be seen from the above two equations that the phase velocity refractive index and code velocity refractive index of order 2 and above are ignored simultaneously in the derivation process. Using this feature, the ionospheric influence on phase and code propagation can be eliminated to the first-order term by using two observation combinations with different frequencies. Considering that satellite altimetry is mainly based on frequency (phase) measurement, therefore, based on the neglect of the second-order term in Eq. (9), the true ranging values $R^{\rm T}$ of each dual frequency are derived as follows:

$$R^{T} = alt_{f_1} - \frac{\int a_1 ds}{f_1^2} + ret_{f_1} + ssb_{f_1} + tro + tide,$$
 (11)

$$R^{T} = alt_{f_2} - \frac{\int a_1 ds}{f_2^2} + ret_{f_2} + ssb_{f_2} + tro + tide,$$
 (12)

where alt_{f_1} , alt_{f_2} , respectively, represent the original ranging value of f_1 , f_2 two frequency bands. ret_{f_1} , ret_{f_2} , respectively, represent the satellite–ground distance correction value after retracking of two frequency bands. ssb_{f_1} , ssb_{f_2} , respectively, represent the sea state bias correction value of two frequency bands.tro represents the tropospheric error correction value, and tide represents the tidal correction value. The quantities irrelevant to the measured frequency band are offset in the process of

difference between Eqs. (11) and (12). After processing, the ionospheric correction value of a certain frequency can be obtained as follows:

$$ion_{f_1} = \frac{(alt_{f_1} + ret_{f_1} + ssb_{f_1}) - (alt_{f_2} + ret_{f_2} + ssb_{f_2})}{(f_1/f_2)^2 - 1}.$$
 (13)

In Eq. (13), ion_{f_1} represents the ionospheric correction value corresponding to the frequency f_1 band. The ionospheric correction model described in Eq. (13) is complete, clear, and convenient for practical calculation of satellite altimetry.

5 Mathematical model of Ka/C/Ku frequency combination for ionosphere error correction to second-order term

Since the Ku/C or Ka/Ku dual frequency combination model has the problems of residual error and resolution reduction in practical application, it is necessary to study the Ku/C/Ka triple frequency combination model in order to further reduce the residual error while correcting the ionosphere to the second-order term in theory. The following analysis focuses on whether the above objectives can be achieved. Under the condition of triple frequency combination, the ionospheric second-order term corrections at each frequency band are obtained as follows:

$$I(f_{ku}) = -\frac{A_1}{f_{ku}^2} - 2\frac{A_2}{f_{ku}^3},\tag{14}$$

$$I(f_{\rm c}) = -\frac{A_1}{f_{\rm c}^2} - 2\frac{A_2}{f_{\rm c}^3},\tag{15}$$

$$I(f_{ka}) = -\frac{A_1}{f_{ka}^2} - 2\frac{A_2}{f_{ka}^3},$$
 (16)

$$A_{1} = \frac{(alt_{ku} - alt_{c} + ret_{ku} + ssb_{ku} - ret_{c} - ssb_{c})f_{ku}^{3}(f_{ka}^{3} - f_{c}^{3})}{f_{ku}^{3}(f_{c} - f_{ka}) + f_{c}^{3}(f_{ka} - f_{ku}) + f_{ka}^{3}(f_{ku} - f_{c})} - \frac{(alt_{c} - alt_{ka} + ret_{c} + ssb_{c} - ret_{ka} - ssb_{ka})f_{ka}^{3}(f_{c}^{3} - f_{ku}^{3})}{f_{ku}^{3}(f_{c} - f_{ka}) + f_{c}^{3}(f_{ka} - f_{ku}) + f_{ka}^{3}(f_{ku} - f_{c})},$$

$$(17)$$

$$A_{2} = -\frac{(alt_{ku} - alt_{c} + ret_{ku} + ssb_{ku} - ret_{c} - ssb_{c})f_{ku}^{3}f_{c}f_{ka}(f_{ka}^{2} - f_{c}^{2})}{f_{ku}^{3}(f_{c} - f_{ka}) + f_{c}^{3}(f_{ka} - f_{ku}) + f_{ka}^{3}(f_{ku} - f_{c})} + \frac{(alt_{c} - alt_{ka} + ret_{c} + ssb_{c} - ret_{ka} - ssb_{ka})f_{ka}^{3}f_{ku}f_{c}(f_{c}^{2} - f_{ku}^{2})}{f_{ku}^{3}(f_{c} - f_{ka}) + f_{c}^{3}(f_{ka} - f_{ku}) + f_{ka}^{3}(f_{ku} - f_{c})}.$$
(18)

Table 2: Ionosphere error order by using Ku/C/Ka frequency combination (m)

Ranging error of each frequency band	Ka/C/Ku combination	1-2 order term correction residual error
Ku: 2.0 cm	f_1 (Ku), f_2 (C), f_3 (Ka)	0.046
Ka: 1.5 cm	f_1 (Ka), f_2 (C), f_3 (Ku)	0.018
C: 6.0 cm	f_1 (C), f_2 (Ku), f_3 (Ka)	1.01
Ku: 1.8 cm	f_1 (Ku), f_2 (C), f_3 (Ka)	0.028
Ka: 1.2 cm	f_1 (Ka), f_2 (c), f_3 (Ku)	0.011
C: 3.6 cm	f_1 (C), f_2 (Ku), f_3 (Ka)	0.64

Table 3: Errors of ionospheric first-order term corrected by different frequency combinations (m)

Ranging error of each frequency band	Frequency combination	lonospheric correction error
$m(\text{alt}_{f_{ki}}) = 2.1 \text{ cm}, \ m(\text{alt}_{f_{ka}}) = 1.0 \text{ cm}, \ m(\text{alt}_{f_c}) = 10.0 \text{ cm},$	Dual frequency $f_1(Ku)$, $f_2(C)$	0.019
$m(\text{ret}_f) = 1.1 \text{ cm}, m(\text{ssb}_f) = 1.8 \text{ cm}$	Dual frequency f_1 (C), f_2 (Ku)	0.13
() <u>-1.2 c,</u> (Dual frequency f_1 (Ka), f_2 (C)	0.002
	Dual frequency f_1 (C), f_2 (Ka)	0.11
	Dual frequency f_1 (Ka), f_2 (Ku)	0.006
	Dual frequency f_1 (Ku), f_2 (Ka)	0.045
$m(\text{alt}_{f_{ki}}) = 1.5 \text{ cm}, \ m(\text{alt}_{f_{ka}}) = 0.7 \text{ cm}, \ m(\text{alt}_{f_c}) = 6.0 \text{ cm},$	Dual frequency f_1 (Ku), f_2 (C)	0.013
$m(\text{ret}_f) = 0.9 \text{ cm}, m(\text{ssb}_f) = 1.8 \text{ cm}$	Dual frequency f_1 (C), f_2 (Ku)	0.082
	Dual frequency f_1 (Ka), f_2 (C)	0.001
	Dual frequency f_1 (C), f_2 (Ka)	0.069
	Dual frequency f_1 (Ka), f_2 (Ku)	0.006
	Dual frequency f_1 (Ku), f_2 (Ka)	0.041

According to the above model, the magnitude of ionospheric residual error under the condition of triple frequency combination is calculated as shown in Table 2.

From the calculation results in Table 2, although the triple frequency combined correction ionosphere is theoretically perfect, its residual error is larger under the same ranging error condition than that under the dual frequency correction mode (if the influence of sea state

deviation error in different frequency bands is considered, the residual error will be larger), which obviously deviates from the original intention of the triple frequency combined theory. Through the analysis of ionosphere, the biggest advantage of using three frequencies for ocean altimetry is not to eliminate the ionosphere, but to give full play to the advantage of dual frequency combination, that is, to use Ku/C combination for ranging in

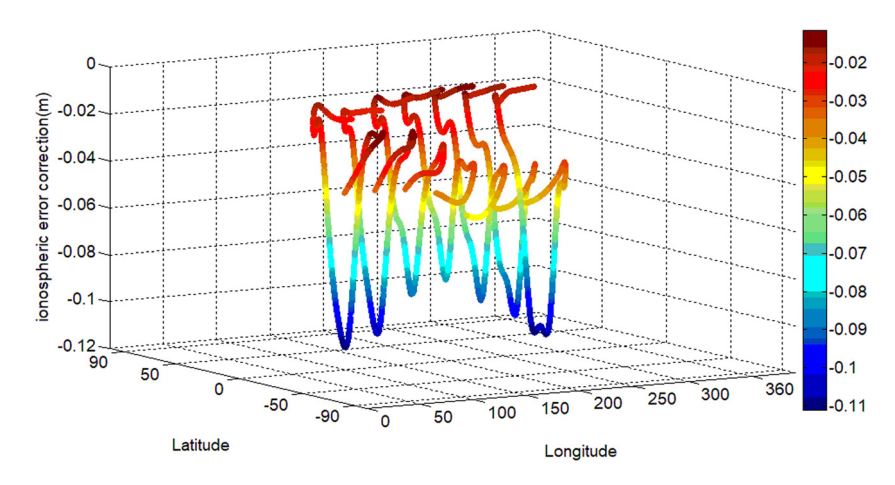


Figure 1: Ionospheric correction by using Ku/C dual frequency data of Jason-2 satellite cycle136 065-072pass.

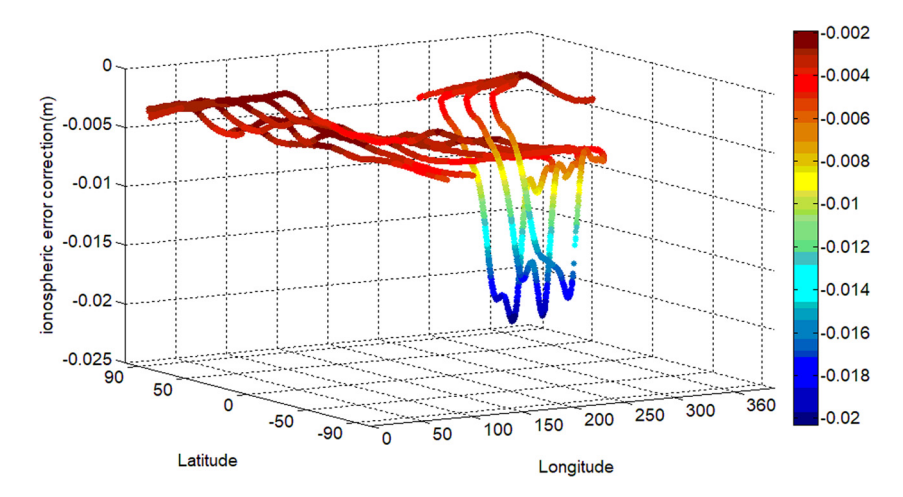


Figure 2: Ionospheric correction of SARAL satellite by using GIM cycle160 004-011pass.

areas with obvious rainfall, and use Ka/C combination for ranging in offshore areas, general sea areas, and ice areas, and to integrate multiple observation measurements in post-processing.

6 Analysis of ranging error of dual frequency combination system

6.1 Theoretical analysis

In theory, the dual frequency correction can completely eliminate the influence of the first-order term of the ionosphere. However, considering that there are still altimeter ranging errors and sea state bias correction errors in engineering practice, there are still some residual errors in the dual frequency correction in actual projects. Based on Eq. (13), the error of the dual frequency ionosphere correction can be derived according to the error propagation law, as shown in the following equation:

assumed that the waveform retracing error for the three frequencies (Ku, Ka, and C) bands is the same, and the sea state deviation correction error for the three frequencies (Ku, Ka, and C) bands is the same too. As the pulse repetition frequency of C-band is lower than that of Ku band, so its theoretical ranging accuracy is about 4–5 times lower than that of Ku band. Therefore, the ranging error of C-band is set to 10 and 6 cm, respectively, in the calculation. The specific results obtained by considering the magnitude of two ranging errors are shown in Table 3.

It can be seen from Table 3 that the Ka/C combination mode is the best one for dual frequency combination and can correct the ionospheric error to be less than 2.5 mm at 1 Hz sampling frequency. The C-band ranging error, regardless of its magnitude, has no significant impact on the Ka/C combined correction ionosphere, but has a significant impact on the Ku/C dual frequency correction ionosphere. When the C-band ranging error is 10 cm, the ionospheric correction error is close to the Ku band ranging error, which obviously reduces the effect of the ionospheric error correction. It is also a solution that has to be used to take

$$m(\text{ion}_{f_1}) = \left| \frac{1}{(f_1/f_2)^2 - 1} \right| \sqrt{m(\text{alt}_{f_1})^2 + m(\text{ret}_{f_1})^2 + m(\text{ssb}_{f_1})^2 + m(\text{alt}_{f_2})^2 + m(\text{ret}_{f_2})^2 + m(\text{ssb}_{f_2})^2}.$$
(19)

In order to compare with Ku frequency band, specific values of dual frequency correction ionospheric error under different combinations of Ku, Ka, and C frequency bands can be calculated based on Eq. (19). On the basis of obtaining ionospheric correction error, the total ranging error under each dual frequency combination can be further calculated according to Eq. (1). During the calculation, the sampling frequency is set to 1 Hz, and it is

the post 100 km scale filtering. If the ionosphere is to be corrected to mm level under the condition of Ku/C dual frequency combination and 1 Hz sampling, the ranging error in C-band needs to be controlled to the same extent as that in Ku band, which is difficult to achieve in theory and engineering. Through the above quantitative analysis, the Ka/C combination form proposed in this study basically eliminates the influence of ionospheric error, and the

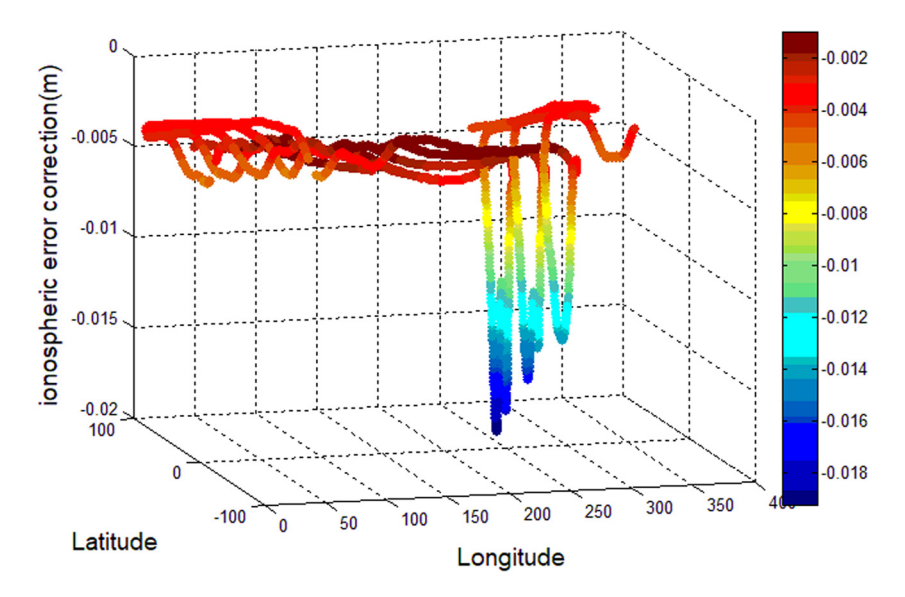


Figure 3: Ionospheric correction of SARAL satellite by using GIM cycle161 004-011pass.

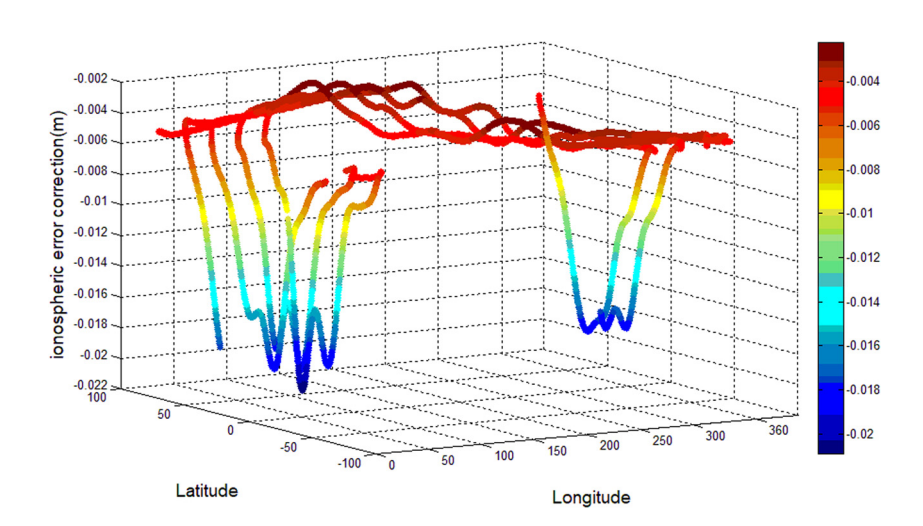


Figure 4: Ionospheric correction of SARAL satellite by using GIM cycle160 020-028 pass.

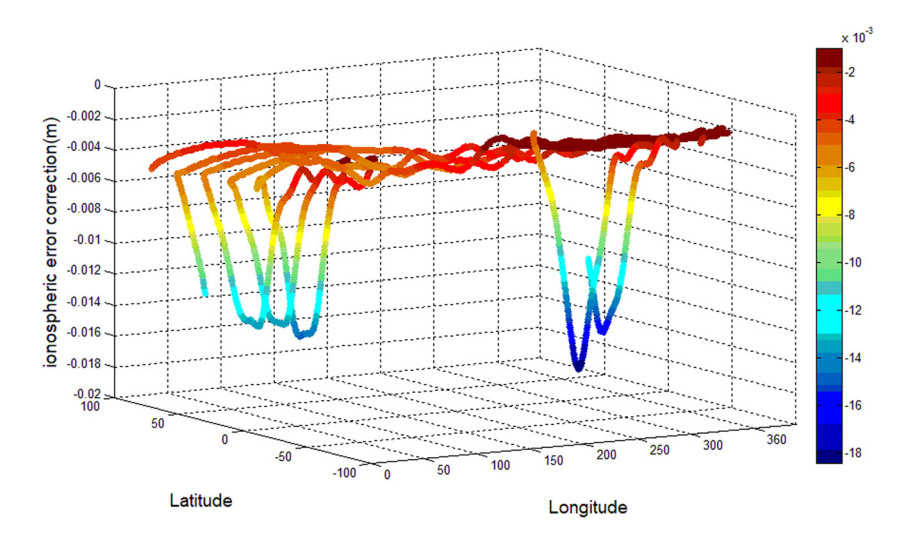


Figure 5: Ionospheric correction of SARAL satellite by using GIM cycle161 020-028 pass.

total accuracy of 1 Hz ranging can be calculated to reach 3.5 cm using Eq. (1).

6.2 Computational analysis of ionospheric correction by using satellite data

In order to validate previous analysis, the altimetry data of the SARAL Satellite and the Jason-2 Satellite are selected for analysis. Among them, the Saral satellite 1 Hz Ka frequency data of the 160 cycle, 161 cycle are used released in April 2022, and the Jason-2 satellite 1 Hz Ku/C dual frequency data of the 136 cycle 065-072 pass are used released in March 2013. The waveform retracking of the above data is based on the Brown model using 4-parameters least squares estimation method (Zhai and Sun 2015), which is consistent with the official processing method of Jason-2 satellite, and the sea state bias adopts the same empirical model as Jason-2 satellite (Labroue et al. 2004). The GIM is used to correct the ionospheric error in the Ka band of the SARAL satellite, and the formula (13) is used to correct the ionospheric error in the Ku/C dual frequency data. The results are shown in Figures 1–5, respectively.

It can be seen from the above figures that the maximum magnitude of ionospheric error correction in Ku band can reach 11 cm, while the maximum magnitude of ionospheric error correction in Ka band can reach 2 cm, which is basically consistent with the theoretical analysis in Section 3. Therefore, for high-precision applications, ionospheric corrections must be made. After Ka/C dual frequency combination is adopted, error correction can be directly conducted without GIM model, and its accuracy will be further improved than GIM model.

7 Conclusion

In this study, according to the characteristics and development trend of satellite altimetry technology, the idea of Ka/C dual frequency combination altimetry system is proposed, that is, to use Ka and C frequency combination forms for high-precision ranging. The dual frequency correction ionospheric first-order term model and correction error are studied in depth. The main conclusions can be summarized as follows:

For the three frequency bands Ka, Ku and C, the error
of the second and third order terms of the single frequency ionospheric correction is below the mm level,
so for the engineering field, which requires in the cm

- level, only the first-order term of the ionospheric correction can be considered.
- 2) For the actual ionospheric correction accuracy of satellite altimetry, the ionospheric error of single frequency ranging must be corrected by other means. Under the condition of dual frequency combination, the ionospheric correction accuracy of Ka/C (35.7 and 5.3 GHz, respectively) combination is the highest, which can reach 3 mm level without filtering. This combination is suitable for general sea areas and ice areas. In areas with obvious rainfall, it needs to be compensated by mathematical models.
- 3) For future satellite altimetry technology, if accurate rainfall models can be used to compensate for the impact of rainfall on Ka band, the Ka/C dual frequency combination system will further improve the applicability of satellite altimetry technology in global sea areas, ice regions, inland lakes, and rivers.

Acknowledgments: Thank you to the editorial department and reviewers for their hard work, and thank you to CNES for providing the satellite data.

Funding information: There is no funding information for this article.

Author contributions: Li Nan: analysis of Ka/C dual frequency correction formulas for ionospheric error; Zhai Zhenhe: analysis of Ka/Ku/C frequency correction formulas for ionospheric error and computation experiment; Ma Jian: collection of ionospheric reference data and study of typical parameters; Guan Bin: collection and preprocessing of SARAL satellite data; Cui Wenhui: collection and preprocessing of Jason-2 satellite data; Li Duan: data drawing and calculation verification.

Conflict of interest: No potential conflict of interest was reported by the authors.

References

Abdalla S, Kolahchi AA, Ablain M, Adusumilli S, Bhowmick SA, Alou-Font E, et al. 2021. Altimetry for the future: Building on 25 years of progress. Adv Space Res. 68(2):319–363. doi: 10.1016/j.asr. 2021.01.022.

Ablain M, Meyssignac B, Zawadzki L, Jugier R, Ribes A, Spada G, et al. 2019. Uncertainty in satellite estimates of global mean

- sea-level changes, trend and acceleration. Earth Syst Sci Data. 11(3):1189-1202. doi: 10.5194/essd-11-1189-2019.
- Azpilicueta F, Nava B. 2021. On the TEC bias of altimeter satellites. J Geod. 95(10):1–15. doi: 10.1007/s00190-021-01564-y.
- Brunner FK, Gu M. 1991. An improved model for the dual frequency ionospheric corection of GPS observations. Manuscr Geod. 16:205–214.
- Borries C, Wilken V, Jacobsen KS, García-Rigo A, Dziak-Jankowska B, Kervalishvili G, et al. 2020. Assessment of the capabilities and applicability of ionospheric perturbation indices provided in Europe. Adv Space Res. 66(3):546-562. doi: 10.1016/j.asr. 2020.04.013.
- Cheng P, Wen H, Liu H, Dong J. 2019. Research situation and future development of satellite geodesy. Geomat Inf Sci Wuhan Univ. 44(1):48–54. doi: 10.13203/j.whugis20180356.
- Denise D, Christian S, Wolfgang B. 2015. Global calibration of SARAL/AltiKa using multi-mission sea surface height cross-overs. Mar Geodesy. 38(Sup1):206-218. doi: 10.1080/01490419.2014.988832.
- Dhote PR, Thakur PK, Domeneghetti A, Chouksey A, Garg V, Aggarwal SP, et al. 2021. The use of SARAL/AltiKa altimeter measurements for multi-site hydrodynamic model validation and rating curves estimation: an application to Brahmaputra river. Adv Space Res. 68(2):691–702. doi: 10.1016/j.asr.2021.05.012.
- Fan C. 2019. Latest advances of global ocean tide models and their accuracy comparisons in coastal areas of China. J Geod Geodyn. 39(5):476–480.
- Ghosh S, Thakur PK, Sharma R, Nandy S, Garg V, Amarnath G, et al. 2017. The potential applications of satellite altimetry with SARAL/AltiKa for Indian inland waters. Proc Natl Acad Sci India Sect A Phys Sci. 87:661–677. doi: 10.1007/s40010-017-0463-5.
- Haoran R, Hongli M. 2013. Effects of inverted barometer correction results on sea state bias. Remote Sens Technol Appl. 28(2):10–16.
- Huang M, Wang R, Zhai G, Ouyang Y. 2007. Integrated data processing for multi-satellite missions and recovery of marine gravity field. Geomat Inf Sci Wuhan Univ. 32(11):988–993.
- Imel DA. 1994. Evaluation of the TOPEX/POSEIDON dual-frequency ionosphere correction. J Geophys Res Ocean. 99(C12):24895-24906. doi: 10.1029/94JC01869.
- Jin T, Hu M, Jiang T, Zhang S. 2012. Cross-calibration errors analysis of ionosphere correction in satellite altimetry. Geomat Inf Sci Wuhan Univ. 37(6):658–661. doi: 10.13203/j.whugis2012.06.013.
- Jing LI, Yue J, Song Y, Peng G. 2016. A new method of offshore waveform retracking using saral altimetry satellite. J Hohai Univ (Nat Sci). 44(4):335–339. doi: 10.3876/j.issn.1000-1980. 2016.04.009.
- Labroue S, Gaspar P, Dorandeu J, Zanife OZ, Mertz F, Vincent P, et al. 2004. Non parametric estimates of the sea state bias for the Jason-1 radar altimeter. Mar Geodesy. 27:(3–4):453–481. doi: 10.1080/01490410490902089.
- Marques HA, Monico JF, Aquino M. 2011. RINEX_HO:Second and third order ionospheric corrections for RINEX observation files. GPS Solut. 15:305–314. doi: 10.1007/s10291-011-0220-1.
- Olivier J, Paul A. 2004. Improved triple-frequency GPS/Galileo carrier phase ambiguity resolution using a stochastic ionosphere modeling. Proceedings of ION,NTM, 01.26-28.
- Pirooznia M, Emadi S, Alamdari M. 2016. The time series spectral analysis of satellite altimetry and coastal tide gauges and tide

- modeling in the coast of Caspian Sea. Open J Mar Sci. 6(2):258-269. doi: 10.4236/ojms.2016.62021.
- Quilfen Y, Chapron B. 2021. On denoising satellite altimeter measurements for high-resolution geophysical signal analysis. Adv Space Res. 68(2):875–891.
- Roblou L, Lamouroux J, Lyard F, Lombard A, Marsaleix P, Mey PD, et al. 2011. Post-processing altimeter data towards coastal applications and integration into coastal models. Coastal Altimetry. Berlin, Heidelberg: Springer. doi: 10.1007/978-3-642-12796-0_9.
- Sandwell DT, Müller RD, Smith WHF, Garcia E, Francis R. 2014.

 New global marine gravity model from CryoSat-2 and Jason-1 reveals buried tectonic structure. Science. 346(6205):65-67. doi: 10.1126/science.1258213.
- Schwatke C, Dettmering D. 2022. Ionospheric corrections for satellite altimetry-impact on global mean sea level trends. Earth Space Sci. 9(4):2333-5084. doi: 10.1029/2021EA002098.
- Tariku YA. 2015. TEC prediction performance of the IRI-2012 model over Ethiopia during the rising phase of solar cycle 24 (2009–2011). Earth Planet Space. 67:140. doi: 10.1186/s40623-015-0312-1.
- Tournadre J, Lambin-Artru J, Steunou N. 2009a. Cloud and rain effects on Altika/Saral Ka-Band radar altimeter-Part I: Modeling and mean annual data availability. IEEE Trans Geosci Remote Sens. 47(6):1806–1817.
- Tournadre J, Lambin-Artru J, Steunou N. 2009b. Cloud and rain effects on AltiKa/SARAL Ka-Band radar altimeter-Part II: Definition of a rain/cloud flag. IEEE Trans Geosci Remote Sens. 47(6):1818–1826.
- Turner JF, Iliffe JC, Ziebart MK. 2013. Global ocean tide models: assessment and use within a surface model of lowest astronomical tide. Mar Geodesy. 36(2):123-137. doi: 10.1080/01490419.2013.771717.
- Verron J, Sengenes P, Lambin J, Noubel J, Steunou N, Guillot A, et al. 2015. The SARAL/AltiKa altimetry satellite mission. Mar Geodesy. 38(SUP.1):2–21. doi: 10.1080/01490419.2014.1000471.
- Vignudelli S, Birol F, Benveniste J, Fu LL, Picot N, Raynal M, et al. 2019. Satellite altimetry measurements of sea level in the coastal zone. Surv Geophys. 40:1319–1349. doi: 10.1007/s10712-019-09569-1.
- Nguyen VS, Pham VT, Van Nguyen L, Andersen OB, Forsberg R, Bui DT. 2020. Marine gravity anomaly mapping for the Gulf of Tonkin area (Vietnam) using Cryosat-2 and Saral/AltiKa satellite altimetry data. Adv Space Res. 66(3):505-519.
- Wang Z, Zhang D, Zhao J, Jin Z, Yun L. 2013. In-orbit calibration and validation of atmospheric correction microwave radiometer on HY-2A satellite. SSCAE. 15(7):44–52.
- Wang Z, Wu Y. 2005. Triple-frequency method for high-order ionospheric refractive error modelling in GPS modemization. J Glob Position Syst. 4(1–2):291–295.
- Yang Q, Yang Y, Wang Z, Song G, Liu Y. 2017. Digital elevation model constructed by GPS and SARAL data over Dome A. Chin J Polar Res. 29(2):204–209. doi: 10.13679/j.jdyj.2017.2.204.
- Zhai Z, Sun Z. 2015. Waveform retracking analysis of Jason-2 altimeter data in the four Chinese sea area. Geomat Inf Sci Wuhan Univ. 40(11):1499–1503. doi: 10.13203/j.whugis20130707.
- Zhang S, Wang X, Huang L, Yin F. 2018. Impact of second order ionosphere delays for GPS kinematic precise point positioning applications. Acta Geod et Cartogr Sin. 47(S0):45–53.